White dwarf binary mergers

An overlooked class of gamma-ray bursts?

Jorge Armando Rueda Hernandez
ICRANet-Ferrara and University of Ferrara

In collaboration with:
Carvalho, G. A.; Coelho, J. G.; de Araujo, J. C .N.; Guidorzi, C.; Loren-Aguilar, P.; Kepler, S. O.; Malheiro, M.; J. F. Rodriguez; Ruffini, R.; Sousa, M. F.

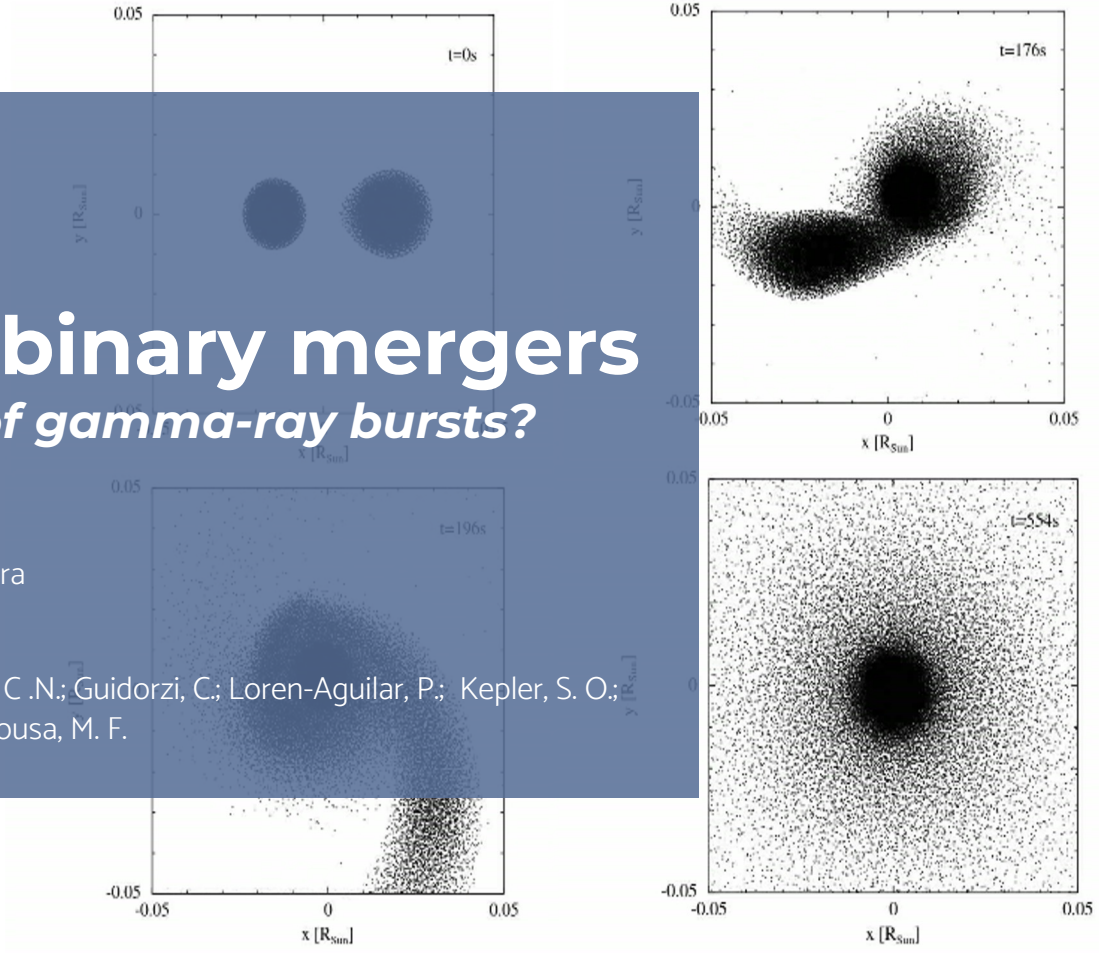

SUMMARY

White dwarf binary (WD-WD) mergers have been studied as formation channels of neutron stars (e.g., magnetars) or type Ia supernovae. But **WD-WD mergers leading to a central WD** (or to a NS by WD collapse, e.g., Yoon et al. 2007; Schwab et al. 2016; Becerra et al. 2018) remnant, might lead to GRBs with a ***precursor/prompt and afterglow emission in the radio, optical, X and gamma-rays***.

This presentation highlights some features of these systems that might be of interest for the GRB community.

SOME RELEVANT FEATURES OF WD-WD MERGERS

WD-WD mergers can lead to type Ia supernovae (double-degenerate scenario), neutron stars/magnetars, and massive, high-field magnetic WDs (**HFMWDs**). ***We are interested in the latter.***

HFMWDs have ***magnetic fields 10^6-10^9 G*** (see, e.g., Kulebi et al. 2009; Ferrario et al. 2015; Kepler et al. 2016, and references therein). They are massive (around M_{sun}) and fast rotating (***tens of seconds of rotation period***). Two recent examples: **SDSS J2211+1136 (1.27 Msun, 70 s period, 15 MG field**; Kilic et al. 2021) and **ZTF J1901+1458 (1.35 Msun, 416 s period, 600-900 MG field**; Caiazzo et al. 2021).

WD-WD are observed systems and the estimated ***merger rate is (4-7)x10^5 Gpc^{-3} yr^{-1}*** (see, e.g., Maoz & Hallakoun 2017; Maoz et al. 2018). This is nearly **10 times larger than the SN Ia rate**. WD-WD systems are main targets for GW space-based detectors like LISA.

But where and which are the products produced by (some of) those mergers?

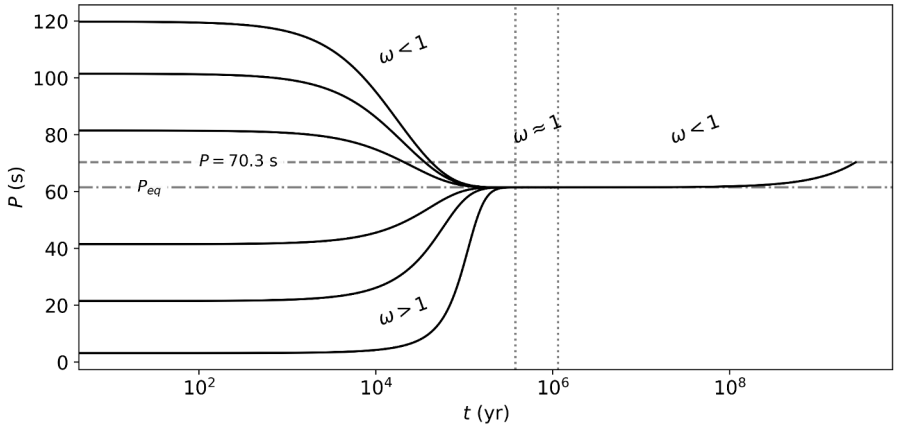

We can "reconstruct" the WD-WD merger progenitor of known HFMWDs. See M. F. Sousa et al. (ApJ, accepted; arXiv: 2208.09506), for J2211+1136 and J1901+1458

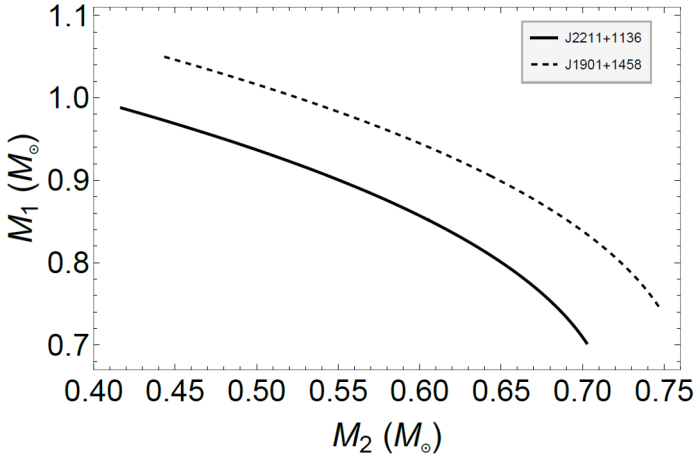

We can also seek for the observational signatures at merger and in the early post-merger life!

Features from DWD merger simulations

Example of an SPH numerical simulation of a 1.1+1.0 solar masses DWD merger

(*see e.g. Rueda et al., JCAP 2019*)

Simulation video courtesy of Pablo Loren-Aguilar

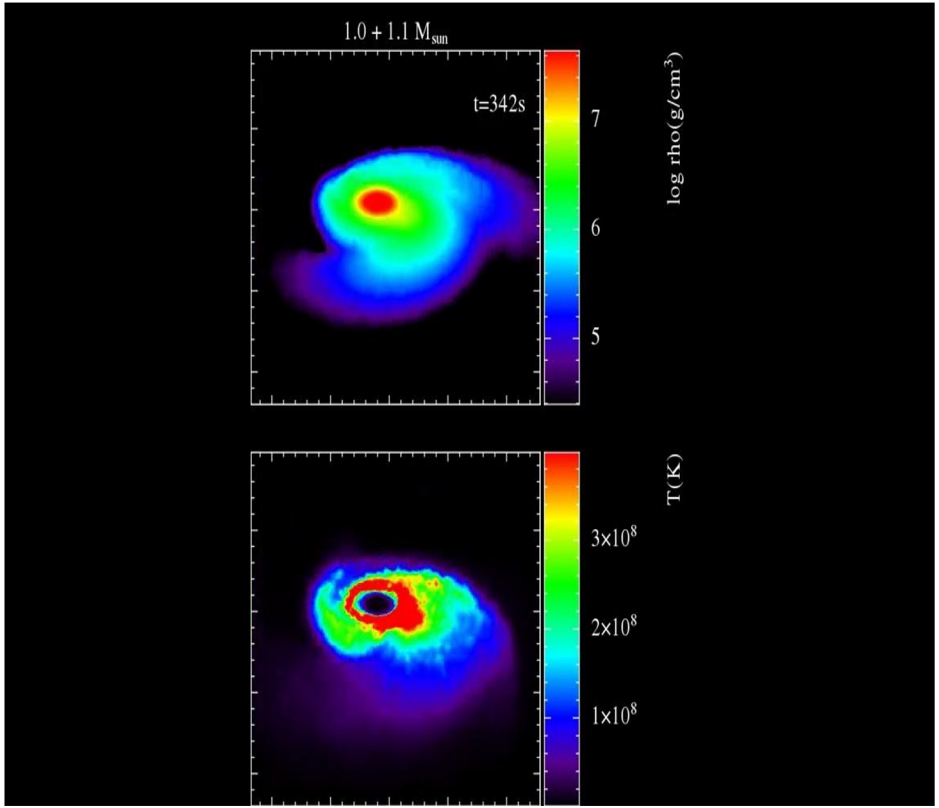

PRE-MERGER CONDITIONS

Numerical simulations of merging binaries: different combinations of mass components leading to different merger fates. Merger timescale, effects of EM emission, precursors, etc.

MERGED CONFIGURATION

Central object + accretion disk + ejecta

What is the nature of the central object? What are the ejecta properties? Accretion disk properties?

POST-MERGER EVOLUTION

Thermal and rotational evolution of the central object.

Evolution of the ejecta (expansion, cooling).

OBSERVATIONAL SIGNATURES

Electromagnetic emission, gravitational wave emission, neutrino emission, interaction with dark matter, etc.
The observational predictions and comparison with observations require an analysis of population too.

Physics at different evolution stages

Observational Signatures

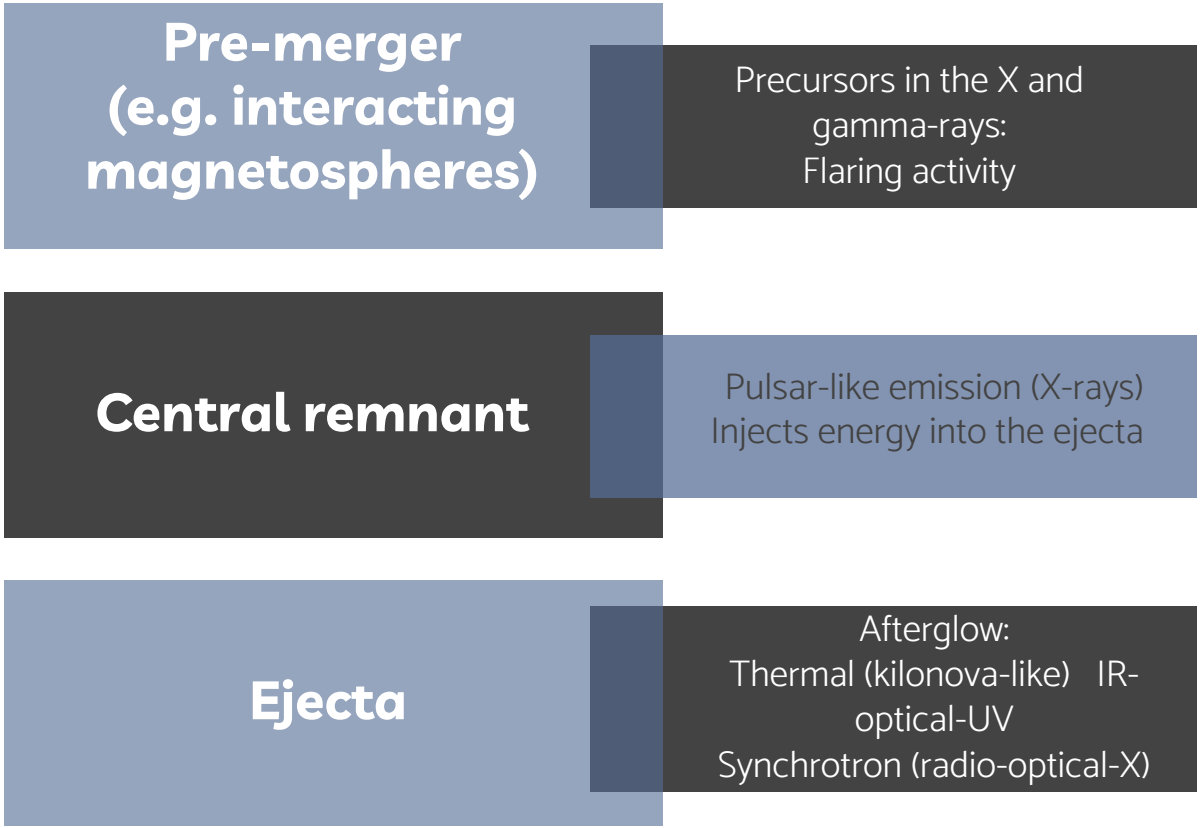

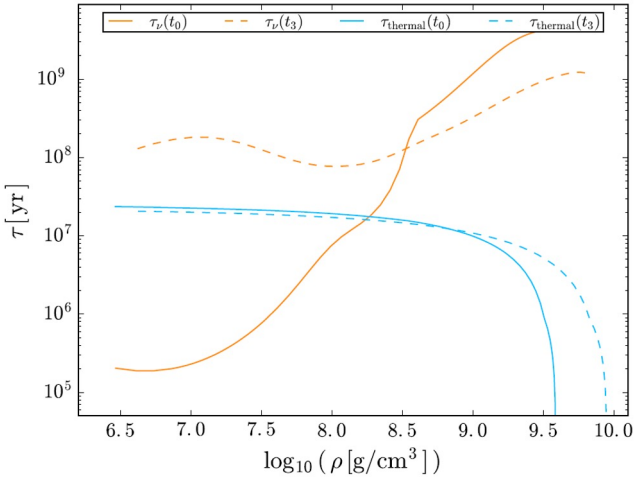

Cooling timescales

Neutrino and thermal cooling timescales in the newborn white dwarf (merged object). They are relevant to determine self-consistently the accretion rate onto the central remnant. Deviations from the Shakura-Sunyaev (alpha) prescription might occur.

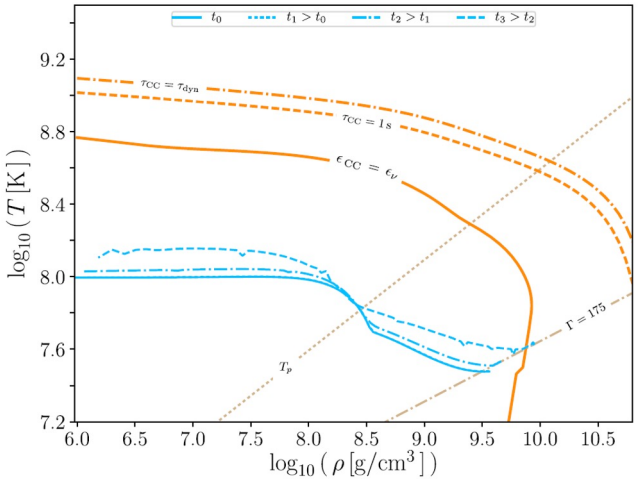

Temperature-density evolution

We must follow the temperature evolution and heating and cooling timescales to determine whether or not explosive (supernova) conditions are achieved..

From Becerra et al., ApJ 2018

We DO NOT want a type Ia supernova

We DO want a stable central remnant

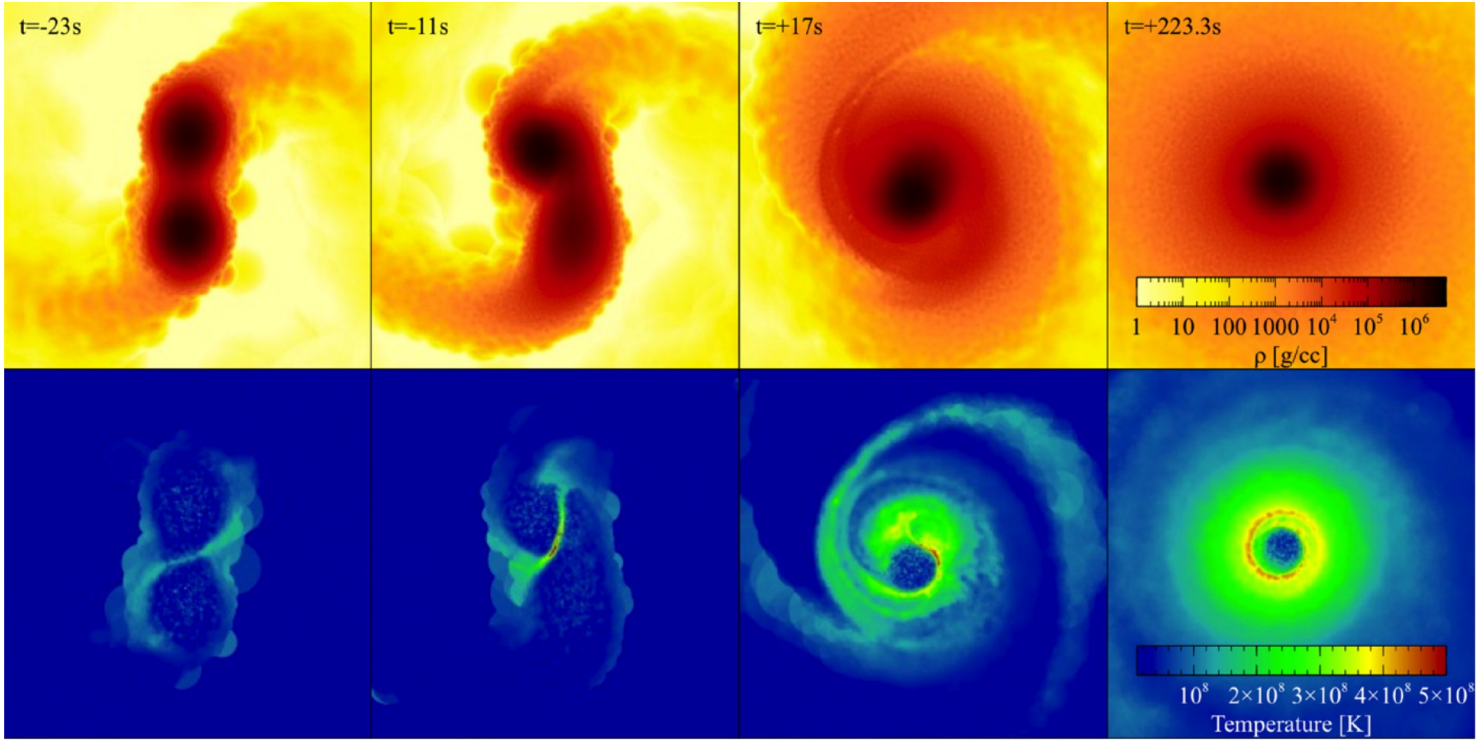

Simulation example taken from Rascusin et al., ApJ 2012

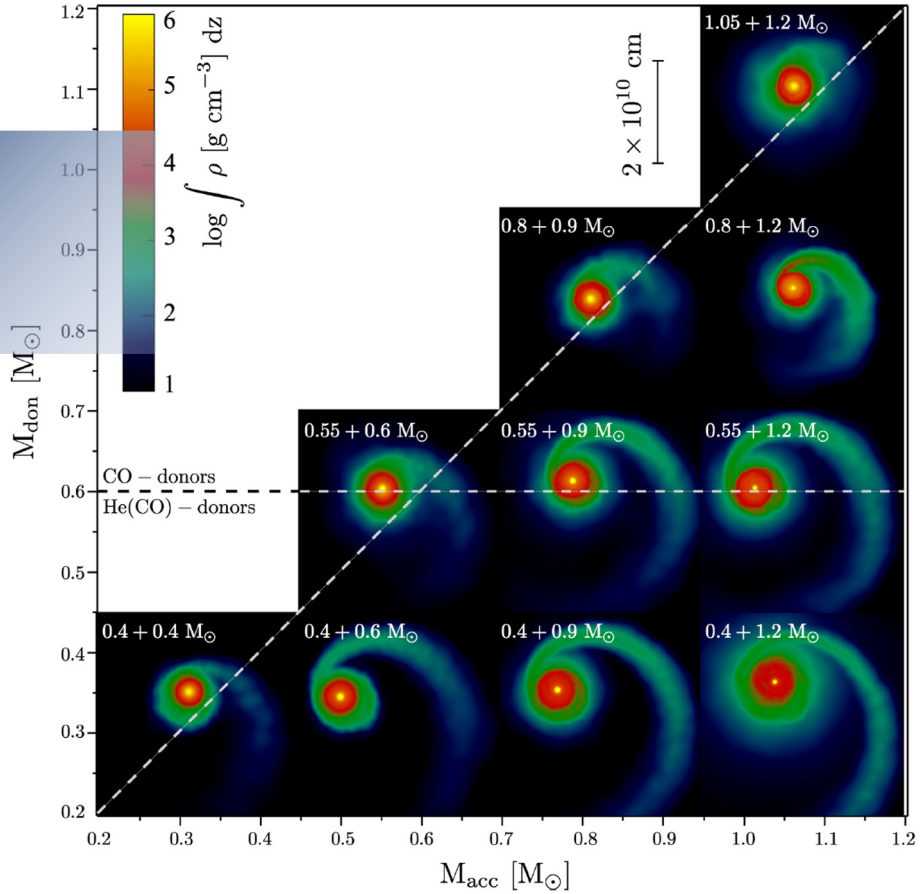

Taken from Dan et al., MNRAS 2014

Pre-merger and post-merger parameter space

$$M_{\rm core} = M_{\rm tot}(0.7786 - 0.5114\,q)$$
$$M_{\rm env} = M_{\rm tot}(0.2779 - 0.464\,q + 0.7161\,q^2)$$
$$M_d = M_{\rm tot}(-0.1185 + 0.9763\,q - 0.6559\,q^2)$$
$$M_{\rm fb} = M_{\rm tot}(0.07064 - 0.0648\,q)$$
$$M_{\rm ej} = \frac{0.0001807\,M_{\rm tot}}{-0.01672 + 0.2463\,q - 0.6982\,q^2 + q^3}$$

Parameter	J2211+1136	J1901+1458
Pre-merger system		
$M_1\ (M_\odot)$	$(0.95, 0.72)$	$(0.98, 0.79)$
$M_2\ (M_\odot)$	$(0.48, 0.70)$	$(0.55, 0.73)$
$M_{\rm tot}\ (M_\odot)$	$(1.43, 1.42)$	$(1.53, 1.52)$
q	$(0.51, 0.97)$	$(0.56, 0.92)$
$M_{\rm ej}\ (10^{-3} M_\odot)$	$(4.26, 0.54)$	$(3.61, 0.69)$
Post-merger system		
$M\ (M_\odot)$	$1.27^{a,b}$	1.35^{c}
R (km)	3210	2140^{c}
P (s)	70.32^{a}	416.20^{c}
$B\ (10^6$ G)	15^{a}	800^{c}
$B_{\rm quad}$ (G)	unconstrained	unconstrained
$M_d\ (M_\odot)$	0.30	0.34
$\dot{M}\ (10^{-7}\ M_\odot\ {\rm s}^{-1})$	$2.60 - 2.68$	$6.92 - 8.05$
$M_{\rm loss}\ (M_\odot)$	0.15	0.17

M. F. Sousa et al. (arXiv: 2208.09506)

Pre-merger/merger: prompt emission

$B = 10^6 - 10^9$ G, Energy budget $= \frac{1}{6} B^2 R^3 = 10^{41} - 10^{47}$ erg , $R = 10^{10}$ cm

The WD pulsar magnetosphere is similar to the one of NSs. The magnetic field and rotation produce an electric field by Faraday (unipolar) induction (Goldreich & Julian 1969).

Numerical simulations show that the merger forms a hot corona of **$T = 10^8 - 10^9$ K** that cools down by neutrinos (e.g., Becerra, et al. 2018). Thermal production of **e+e- pairs** can occur. Charged particles accelerated by the electric field produce curvature and synchrotron radiation. Photon-photon collisions can lead to a pair-plasma. The photons able to escape and the transparency of the plasma can lead to a non-thermal + thermal emission at energies from hard X-rays to gamma-rays. This is similar to soft gamma repeaters flares.

Similar to the GRB prompt emission of traditional models! Flares can release similar energies from the crack of twisted field lines at merger (see also the flares in Malheiro et al. 2012 in the WD model of magnetars). We need simulations to confirm whether or not they indeed occur!

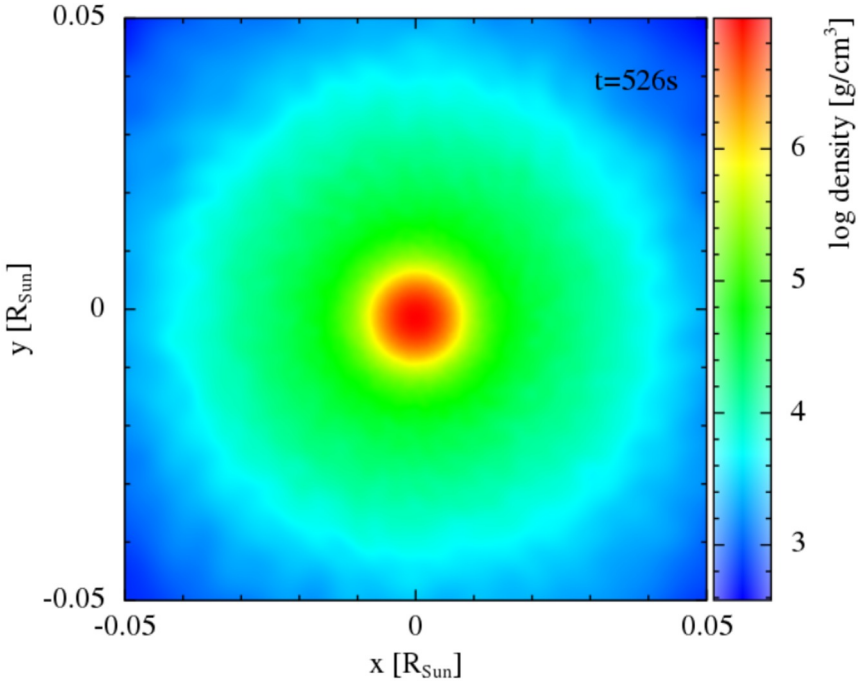

Early afterglow from the cooling ejecta

Velocity	Mass	Magnetic field	Energy injection
0.01 c (front)	10^{-3} M_{sun}	newborn WD field decreasing with r (e.g., powerlaw)	newborn WD pulsar, thermal energy, nuclear energy, etc.

Figure from Rueda et al. ICAP 2019

Ejecta expansion and cooling: early "kilonova-like" emission

Rueda et al., JCAP 2018, 2019

$$r_i(t) = r_{i,0}\hat{t}^n, \quad v_i(t) = n\frac{r_i(t)}{t} = v_{i,0}\hat{t}^{n-1}$$

$$\rho(r_i) = \frac{(3-m)}{4\pi}\frac{m_{\rm ej}}{R_{*,0}^3}\left[\left(\frac{R_{\rm max}}{R_*}\right)^{3-m} - 1\right]^{-1}\left(\frac{r_i}{R_*}\right)^{-m}\hat{t}^{-3n}$$

$$\dot{E}_i = -P_i\,\dot{V}_i - L_{{\rm cool},i} + H_{{\rm inj},i}$$

$$E_i = 3P_i\,V_i + L^{\rm abs}_{{\rm cool},i}\frac{r_i}{c}$$

$$\sum_{j=1}^{N} m_j = m_{\rm ej} \qquad L_{{\rm cool},i} \approx \frac{cE_i}{r_i(1+\tau_{{\rm opt},i})}$$

$$\tau_{\rm opt,i} = \int_{\infty}^{r_i}\kappa\rho(r)dr = \int_{R_{\rm max}}^{r_i}\kappa\rho(r)dr = \tau_{i,0}\hat{t}^{-2n}$$

$$\tau_{i,0} \equiv \frac{m-3}{m-1}\frac{\kappa m_{\rm ej}}{4\pi R_{*,0}^2}\frac{\left[\left(\frac{R_*}{r_i}\right)^{m-1} - \left(\frac{R_*}{r_{\rm max}}\right)^{m-1}\right]}{\left[1-\left(\frac{R_*}{R_{\rm max}}\right)^{m-3}\right]}$$

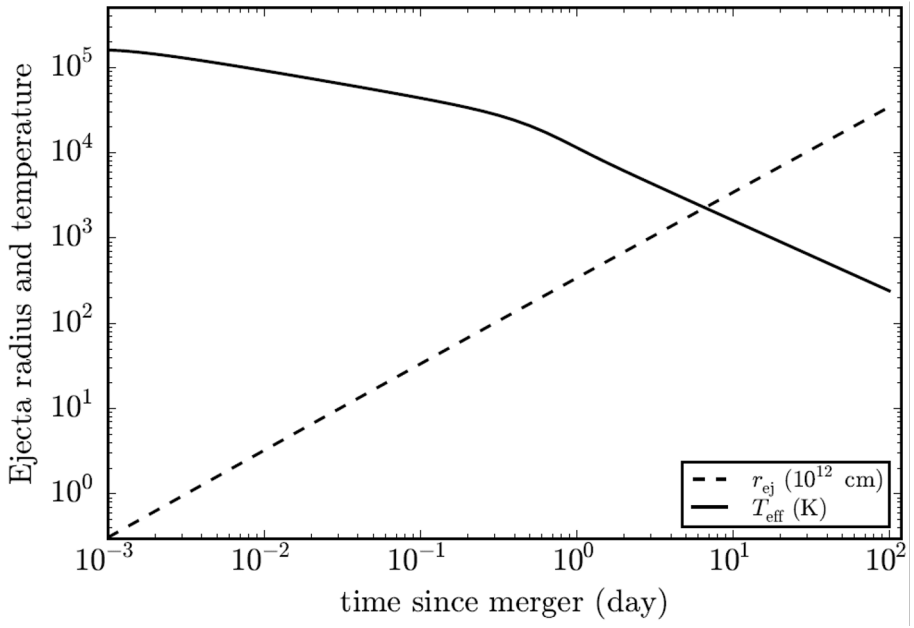

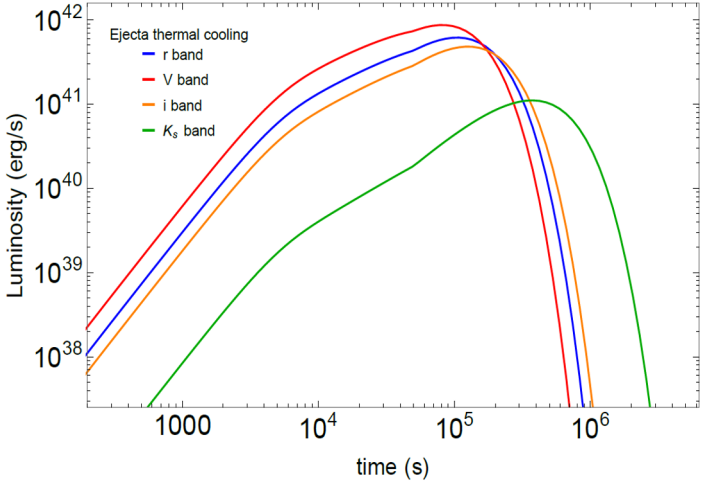

Spectrum

Spectral density flux of the blackbody produced by the "kilonova-like" emission by the cooling of the expanding ejecta

$$R_{\rm ph} = \frac{R_{\rm max,0}\hat{t}^n}{\left[1+\frac{m-1}{m-3}\frac{4\pi R_{*,0}^2}{\kappa m_{\rm ej}}\frac{\left[1-\left(\frac{R_*}{R_{\rm max}}\right)^{m-3}\right]}{\left(\frac{R_{\rm max}}{R_*}\right)^{m-1}}\hat{t}^{2n}\right]^{\frac{1}{m-1}}}$$

$$\hat{t}_{{\rm tr},*} = \left\{\frac{m-3}{m-1}\frac{\kappa m_{\rm ej}}{4\pi R_{*,0}^2}\left(\frac{R_*}{R_{\rm max}}\right)^{m-1}\frac{\left[\left(\frac{R_{\rm max}}{R_*}\right)^{m-1}-1\right]}{\left[1-\left(\frac{R_*}{R_{\rm max}}\right)^{m-3}\right]}\right\}^{\frac{1}{2n}}$$

$$L_{\rm bol} = \sum_{j=1}^{N} L_{{\rm cool},j} \qquad T_s = \left(\frac{L_{\rm bol}}{4\pi R_{\rm ph}^2\sigma}\right)^{1/4} \qquad B_\nu(\nu,t) = \frac{2\pi h\nu^3}{c^2}[e^{\frac{h\nu}{k_b T_s(t)}}-1]^{-1}$$

$$J_{\rm cool}(\nu,t) = 4\pi R_{\rm ph}^2(t) B_\nu(\nu,t) \qquad L_{\rm cool}(\nu_1,\nu_2;t) = \int_{\nu_1}^{\nu_2} J_{\rm cool}(\nu,t)d\nu$$

Rueda et al., JCAP 2019; Rueda et al., IJMPD 2022

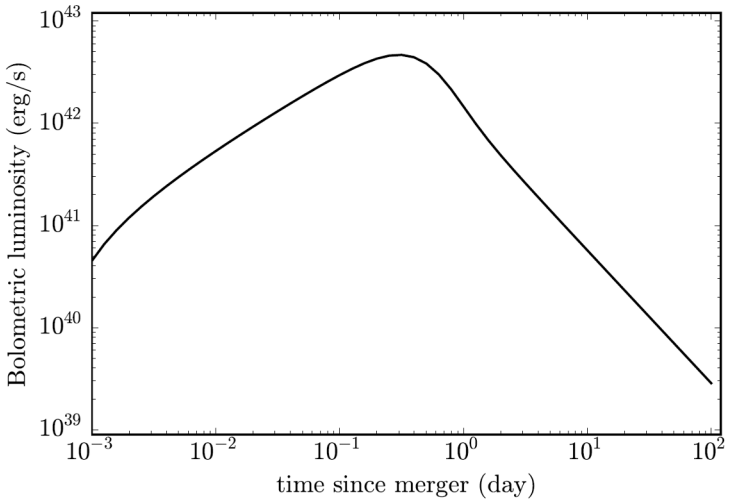

OBSERVABILITY

EARLY AFTERGLOW:

Example: for a follow-up at a limiting magnitude ***M=22, 10^{40} - 10^{41} erg/s*** leads to a maximum detectability distance of ***50-150 Mpc.***

This leads to a detection rate of ***10-10^{3} events/yr.***

Where are they?

Can these transients be sources we are detecting? cow-like (FOTs, FBOTs), FRBs (e.g., Margalit, Berger and Metzger, 2019), luminous red novae, etc.?

$$L_{\mathrm{syn},\nu} = \int_1^{\gamma_{\max}} N(\gamma, t) P_{\mathrm{syn}}(\nu, \gamma) d\gamma$$

$$P_{\mathrm{syn}}(\nu, \gamma) = \sqrt{3} \frac{e^2}{c} \omega_{\mathrm{gyr}} \sin\alpha \, F(x)$$

$$\omega_{\mathrm{gyr}} = 2\pi\nu_{\mathrm{gyr}} = \frac{eB}{m_e c}$$

Synchrotron (afterglow) emission

Rueda, J. A., et al., IJMPD 2022; arXiv: 2202.00314
Rueda, J. A., AIP Conf. Proc.; arXiv: 2202.00316

Kinetic equation

$$\frac{\partial N(E,t)}{\partial t} = -\frac{\partial}{\partial E}\left[\dot{E}\, N(E,t)\right] + Q(E,t)$$

General solution

$$N(E,t) = \int_E^{\infty} Q[E_i, t_i(t, E_i, E)] \frac{\partial t_i}{\partial E} dE_i$$

$$-\dot{E} = \frac{E}{\tau_{\rm exp}} + \beta B_*(t)^2 E^2$$

$$Q(E,t) = Q_0(t) E^{-\gamma}, \qquad 0 \le E \le E_{\rm max}$$

$$L_{\rm inj}(t) = L_0 \left(1 + \frac{t}{t_q}\right)^{-k}$$

$$B_i(t) = B_{i,0} \left[\frac{r_{i,0}}{r_i(t)}\right]^{\mu} = \frac{B_{i,0}}{\hat{t}^{\mu n}} \qquad E = \frac{E_i \, (t_i/t)^n}{1 + \mathcal{M} E_i t_i^n \left[\frac{1}{\hat{t}_i^{\,n(1+2\mu)-1}} - \frac{1}{\hat{t}^{\,n(1+2\mu)-1}}\right]} \qquad \mathcal{M} \equiv \frac{\beta B_{*,0}^2 t_*^{1-n}}{n(1+2\mu)-1}$$

Approx. solution

$$N(E,t) \approx \begin{cases} \dfrac{q_0}{\beta B_{*,0}^2 (\gamma-1)} \hat{t}^{2\mu n} E^{-(\gamma+1)}, & t < t_q \\ \dfrac{q_0}{\beta B_{*,0}^2 (\gamma-1)} \left(\dfrac{t_q}{t_*}\right)^k \hat{t}^{2\mu n - k} E^{-(\gamma+1)}, & t_q < t < t_b \end{cases}$$

Synchrotron (afterglow) emission

Rueda, J. A., et al., IJMPD 2022; arXiv: 2202.00314
Rueda, J. A., AIP Conf. Proc.; arXiv: 2202.00316

$$\nu \approx \nu_{\rm crit} \approx \alpha B E^2$$

$$P_{\rm syn}(\nu, E) \approx P_{\rm syn}(\nu) = \beta B_*^2 E^2(\nu) = \frac{\beta}{\alpha} B_* \nu$$

$$J_{\rm syn}(\nu, t) = \frac{\beta}{2} \alpha^{\frac{p-3}{2}} \eta B_{*,0}^{\frac{p+1}{2}} \hat{t}^{\frac{2l-\mu n(p+1)}{2}} \nu^{\frac{1-p}{2}}$$

Synchrotron (afterglow) emission

Rueda, J. A., et al., IJMPD 2022; arXiv: 2202.00314
Rueda, J. A., AIP Conf. Proc.; arXiv: 2202.00316

$$N(E, t) = \eta \hat{t}^l E^{-p}$$

$$L_{\rm syn}(\nu_1, \nu_2; t) = \int_{\nu_1}^{\nu_2} J_{\rm syn}(\nu, t) d\nu$$

$$J_{\rm syn}(\nu, t) = \frac{\beta}{2} \alpha^{\frac{p-3}{2}} \eta B_{*,0}^{\frac{p+1}{2}} \hat{t}^{\frac{2l-\mu n(p+1)}{2}} \nu^{\frac{1-p}{2}}$$

$$L_{\rm syn}(\nu, t) \approx \nu J_{\rm syn}(\nu, t) = \frac{\beta}{2} \alpha^{\frac{p-3}{2}} \eta B_{*,0}^{\frac{p+1}{2}} \hat{t}^{\frac{2l-\mu n(p+1)}{2}} \nu^{\frac{3-p}{2}}$$

Luminosity at different wavelengths

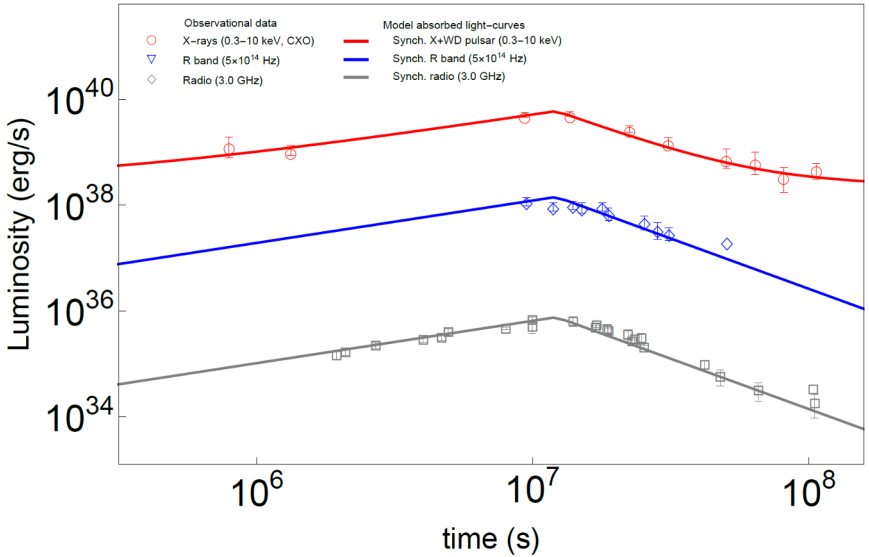

Synchrotron afterglow: GRB 170817A-like emission

The synchrotron radiation from the ejecta expanding in the magnetic field of the central remnant might lead to a multiwavelength (X-optical-radio) afterglow emission similar to the one of GRB 170817A. There is also emission at higher energies (e.g. hard X and gamma-rays) depending on the currently unconstrained maximum electron energy.

From Rueda et al., IJMPD 2022; arXiv: 2202.00314

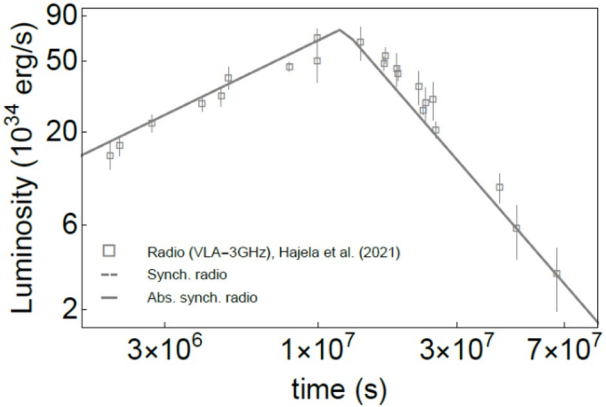

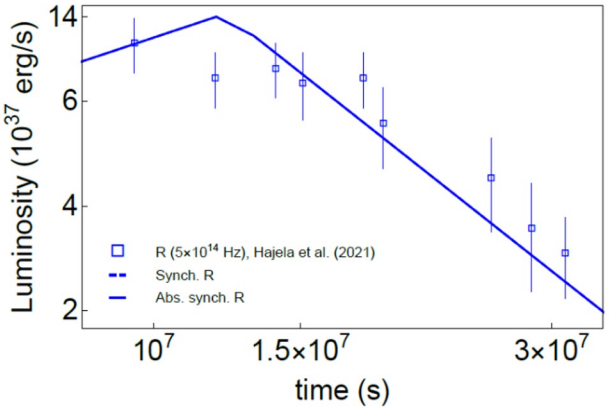

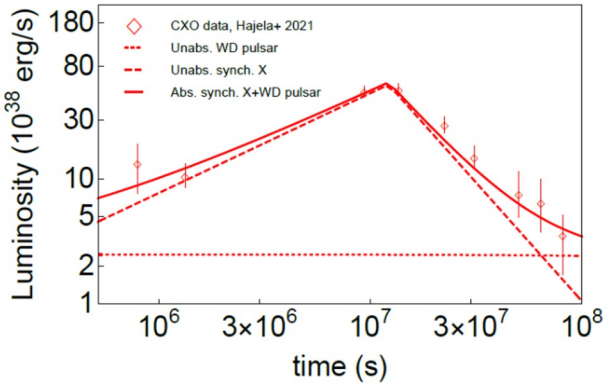

OBSERVABILITY (by some future missions)

PROMPT EMISSION: 10^{46} erg/s at 50 Mpc leads to a flux at earth of 10^{-8} erg/s/cm^2. This is detectable by the SXI and/or XGIS of **THESEUS (upper and lower left)**. For a merger rate 10^5-10^6 Gpc^{-3} yr^{-1}, the detection rate is ***10-100 events/yr***.

LATE AFTERGLOW: 10^{40} erg/s at 10 Mpc translate in a flux at earth of 10^{-13} erg/s/cm^2. This is detectable in the soft X-rays by the SXI of **THESEUS** for exposure times > 10^5 s. The detection rate is ***0.1-1 events/yr.*** This is also detectable by the NFT of **ASTENA (lower right)** at 50-600 keV with a similar detection rate (assuming a comparable flux).

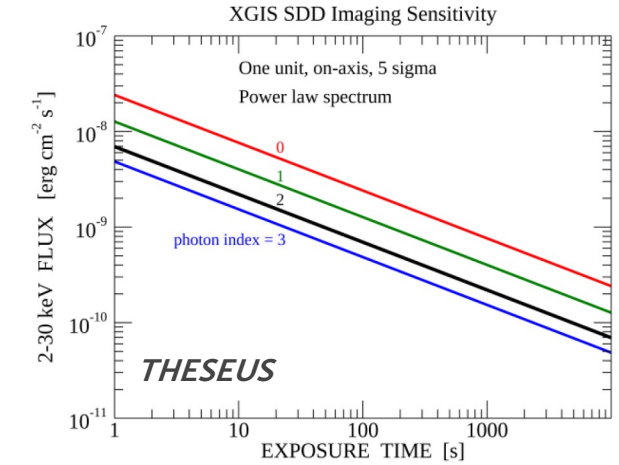

Amati, L., et al., 2021

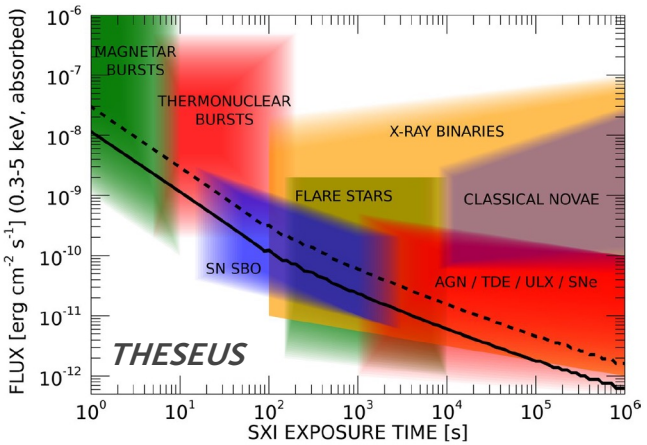

Mereghetti, S., et al. 2021

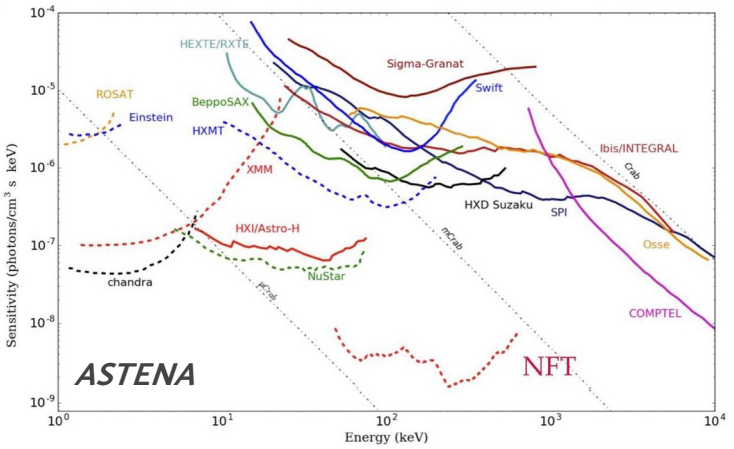

Frontera, F., et al. 2021

Gravitational Waves

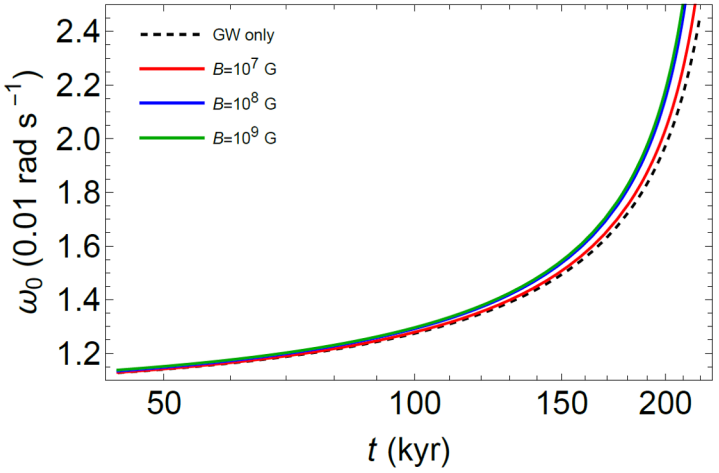

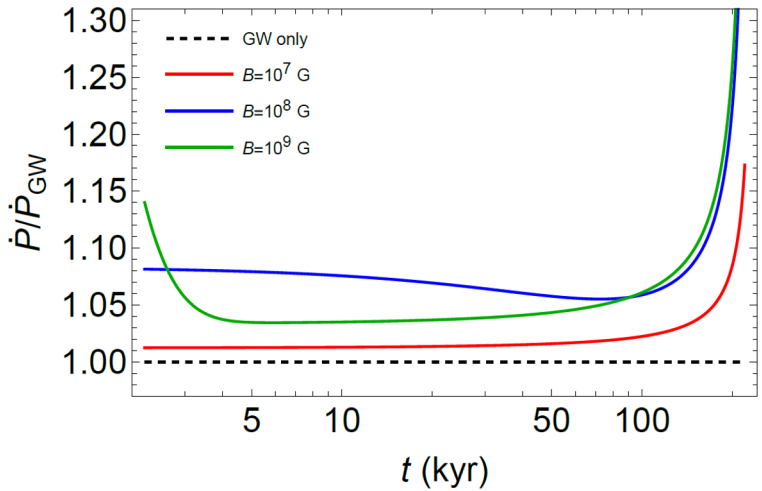

WD-WD are targets for space-based GW detectors like LISA. They will transit the detector for long time (years) accumulating huge signal-to-noise ratio. Tracking and modeling them with high accuracy allow to predict merger times and probe physical ingredients like magnetic fields. See e.g. Carvalho, G. A. et al. ApJ, accepted; arXiv: 2208.00863.; also Wu et al. 2002, Dall'Osso et al. 2006, Lai 2012.

Post-merger EM observations will confirm or dismiss GW models. There will be no ground-based (kHz) GW counterpart.

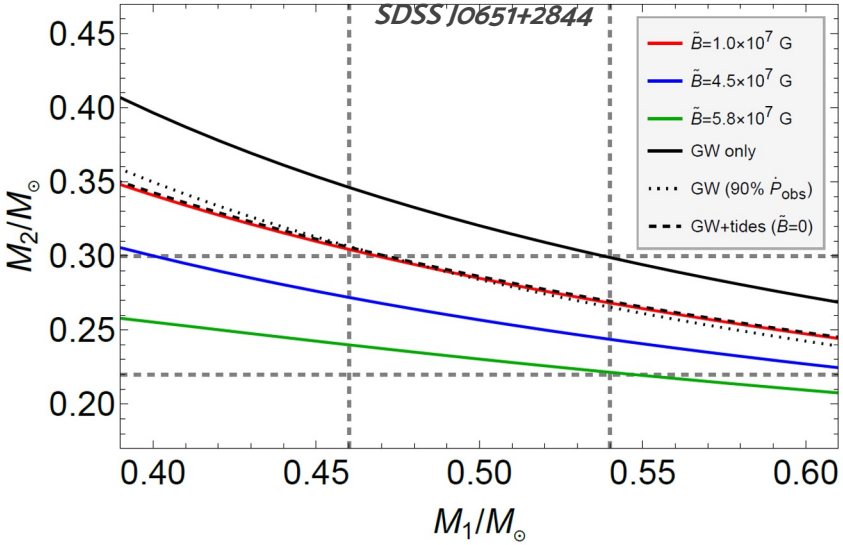

CONCLUSION

Precursor/Prompt

10^{46} erg emitted in a second, so 10^{46} erg/s at merger times for magnetic fields of 10^{9} G.

Early afterglow: “kilonova-like”

10^{40} - 10^{42} erg/s from the ejecta cooling in the IR-optical-UV bands at 0.5-1 day post-merger.

Late afterglow

10^{39} - 10^{40} erg/s of synchrotron radiation in the X-gamma rays at days-months post-merger. Optical and radio counterparts.

Very-late afterglow

Pulsar-like emission (magnetar-like) from the newborn central remnant. Decaying power-law from 10^{39} erg/s at months/year post-merger.

THANKS

Questions?

Contact:
jorge.rueda@icra.it
jorge.ruedah@gmail.com

CREDITS

This is where you give credit to the ones who are part of this project.

- Presentation template by Slidesgo
- Icons by Flaticon
- Infographics by Freepik
- Images created by Freepik